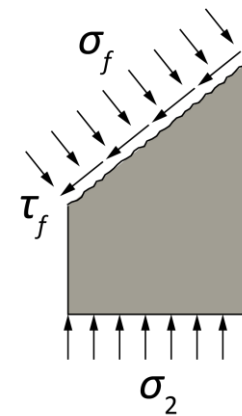
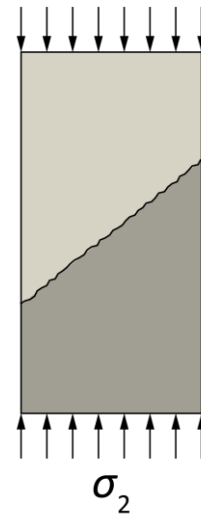
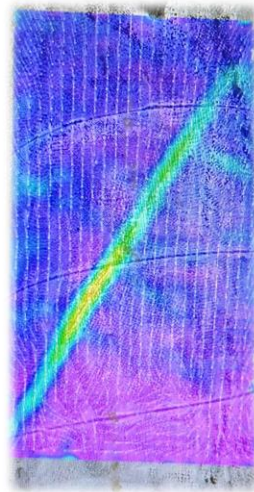
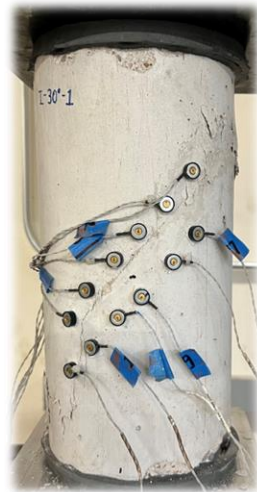


# INVESTIGATING INTERFACE SHEAR RESISTANCE THROUGH SLANT SHEAR TESTS: A CRITICAL REVIEW OF CURRENT DESIGN CODES

Brandon Li, Andrea Campos Sanchez

Dennis Wang, Yongjae Yu, Anca Ferche, Oguzhan Bayrak



# OUTLINE

INTRODUCTION

EXPERIMENTAL  
PROGRAM

CODE  
EVALUATION

DATABASE  
ANALYSIS

CONCLUSIONS



# INTRODUCTION

“Cities are not static – they are growing”

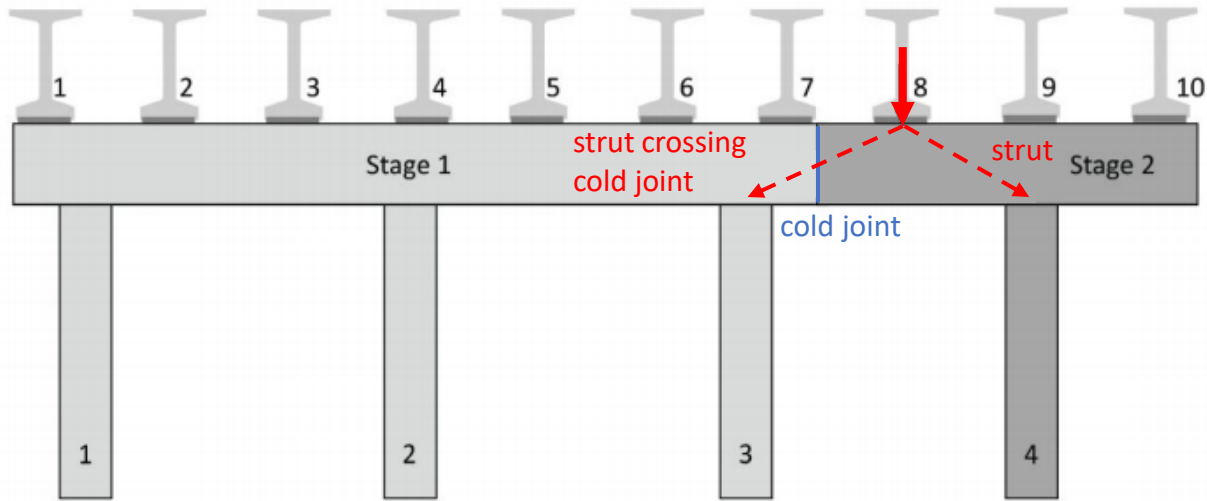


THE WORLD'S GATHERING PLACE FOR ADVANCING CONCRETE

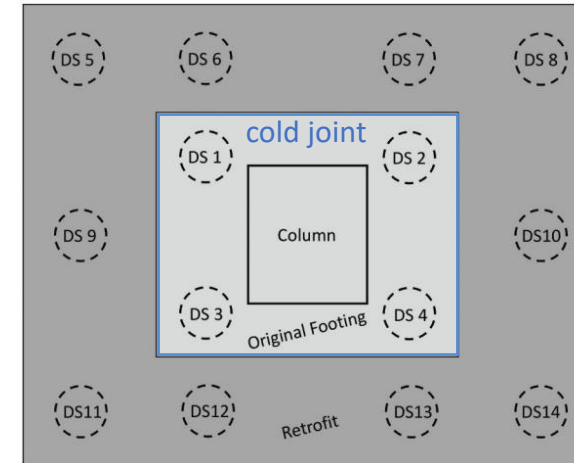
aci CONCRETE  
CONVENTION



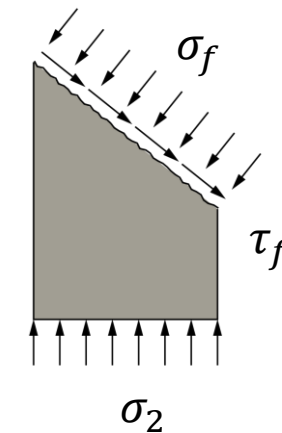
# INTRODUCTION



Strut Crossing Cold Joint in Stage Construction (Bayrak, 2020)



Strut Crossing Cold Joint in Retrofitted Pier Cap (Bayrak, 2020)



# EXPERIMENTAL PROGRAM

## Test Matrix – Series I: Angle

Series	Groups	Angle (°)	Interface Roughness	Concrete Strength	Casting Age	Agg. Size
I-Angle	I-30	30	R1	N-N	3 days	A1-A1
	I-38	38	R1	N-N	3 days	A1-A1
	I-45	45	R1	N-N	3 days	A1-A1
	I-60	60	R1	N-N	3 days	A1-A1
II-Interface Roughness	II-M	-	M	N-N	3 days	A1-A1
	II-NR	30	NR	N-N	3 days	A1-A1
	II-R1	30	R1	N-N	3 days	A1-A1
	II-R2	30	R2	N-N	3 days	A1-A1
III-Concrete Strength	III-H1	30	R1	N-H1	3 days	A1-A1
	III-H2	30	R1	N-H2	3 days	A1-A1
IV-Casting Age	IV-1/6	30	R1	N-N	4 hours	A1-A1
	IV-28	30	R1	N-N	28 days	A1-A1
	IV-56	30	R1	N-N	56 days	A1-A1
V-Aggregate Size	V-A2	30	R1	N-N	3 days	A1-A2
	V-A3	30	R1	N-N	3 days	A1-A3



30°



38°



45°



60°

# EXPERIMENTAL PROGRAM

## Test Matrix – Series II: Interface Roughness

Series	Groups	Angle (°)	Interface Roughness	Concrete Strength	Casting Age	Agg. Size
I-Angle	I-30	30	R1	N-N	3 days	A1-A1
	I-38	38	R1	N-N	3 days	A1-A1
	I-45	45	R1	N-N	3 days	A1-A1
	I-60	60	R1	N-N	3 days	A1-A1
II-Interface Roughness	II-M	-	M	N-N	3 days	A1-A1
	II-NR	30	NR	N-N	3 days	A1-A1
	II-R1	30	R1	N-N	3 days	A1-A1
	II-R2	30	R2	N-N	3 days	A1-A1
III-Concrete Strength	III-H1	30	R1	N-H1	3 days	A1-A1
	III-H2	30	R1	N-H2	3 days	A1-A1
IV-Casting Age	IV-1/6	30	R1	N-N	4 hours	A1-A1
	IV-28	30	R1	N-N	28 days	A1-A1
	IV-56	30	R1	N-N	56 days	A1-A1
V-Aggregate Size	V-A2	30	R1	N-N	3 days	A1-A2
	V-A3	30	R1	N-N	3 days	A1-A3



NR



R1

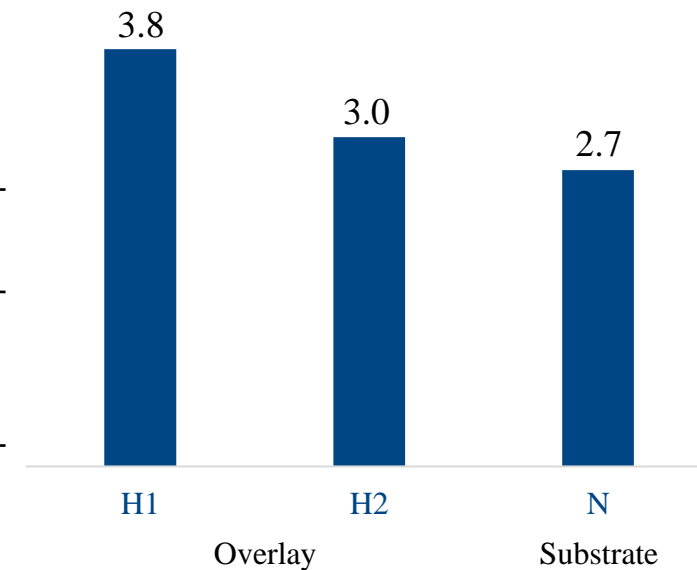


R2

# EXPERIMENTAL PROGRAM

## Test Matrix – Series III: Variation in Concrete Strength

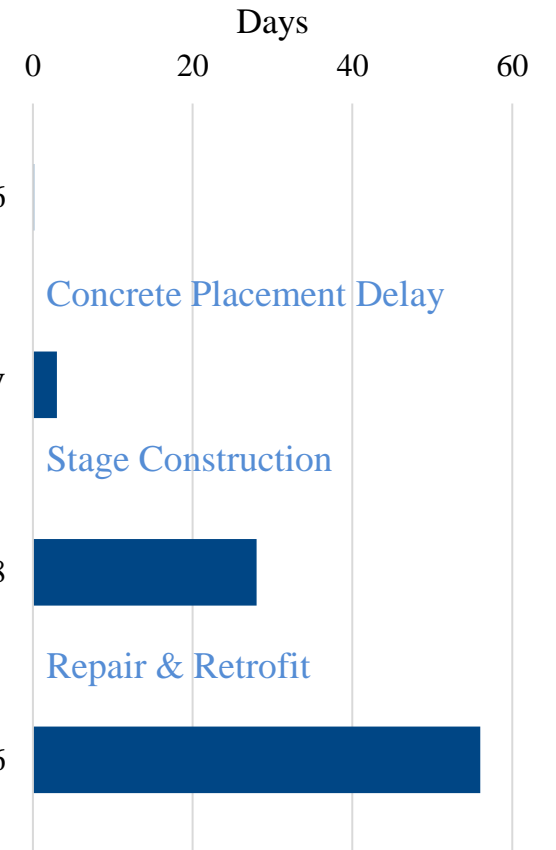
Series	Groups	Angle (°)	Interface Roughness	Concrete Strength	Casting Age	Agg. Size
I-Angle	I-30	30	R1	N-N	3 days	A1-A1
	I-38	38	R1	N-N	3 days	A1-A1
	I-45	45	R1	N-N	3 days	A1-A1
	I-60	60	R1	N-N	3 days	A1-A1
II-Interface Roughness	II-M	-	M	N-N	3 days	A1-A1
	II-NR	30	NR	N-N	3 days	A1-A1
	II-R1	30	R1	N-N	3 days	A1-A1
	II-R2	30	R2	N-N	3 days	A1-A1
III-Concrete Strength	III-H1	30	R1	N-H1	3 days	A1-A1
	III-H2	30	R1	N-H2	3 days	A1-A1
IV-Casting Age	IV-1/6	30	R1	N-N	4 hours	A1-A1
	IV-28	30	R1	N-N	28 days	A1-A1
	IV-56	30	R1	N-N	56 days	A1-A1
V-Aggregate Size	V-A2	30	R1	N-N	3 days	A1-A2
	V-A3	30	R1	N-N	3 days	A1-A3



# EXPERIMENTAL PROGRAM

## Test Matrix – Series IV: Casting Age Difference

Series	Groups	Angle (°)	Interface Roughness	Concrete Strength	Casting Age	Agg. Size	
I-Angle	I-30	30	R1	N-N	3 days	A1-A1	IV-1/6
	I-38	38	R1	N-N	3 days	A1-A1	
	I-45	45	R1	N-N	3 days	A1-A1	
	I-60	60	R1	N-N	3 days	A1-A1	
II-Interface Roughness	II-M	-	M	N-N	3 days	A1-A1	I,II,III,V
	II-NR	30	NR	N-N	3 days	A1-A1	
	II-R1	30	R1	N-N	3 days	A1-A1	
	II-R2	30	R2	N-N	3 days	A1-A1	
III-Concrete Strength	III-H1	30	R1	N-H1	3 days	A1-A1	IV-28
	III-H2	30	R1	N-H2	3 days	A1-A1	
IV-Casting Age	IV-1/6	30	R1	N-N	4 hours	A1-A1	IV-56
	IV-28	30	R1	N-N	28 days	A1-A1	
	IV-56	30	R1	N-N	56 days	A1-A1	
V-Aggregate Size	V-A2	30	R1	N-N	3 days	A1-A2	
	V-A3	30	R1	N-N	3 days	A1-A3	





# EXPERIMENTAL PROGRAM

## Test Matrix – Series V: Aggregate Size

Series	Groups	Angle (°)	Interface Roughness	Concrete Strength	Casting Age	Agg. Size
I-Angle	I-30	30	R1	N-N	3 days	A1-A1
	I-38	38	R1	N-N	3 days	A1-A1
	I-45	45	R1	N-N	3 days	A1-A1
	I-60	60	R1	N-N	3 days	A1-A1
II-Interface Roughness	II-M	-	M	N-N	3 days	A1-A1
	II-NR	30	NR	N-N	3 days	A1-A1
	II-R1	30	R1	N-N	3 days	A1-A1
	II-R2	30	R2	N-N	3 days	A1-A1
III-Concrete Strength	III-H1	30	R1	N-H1	3 days	A1-A1
	III-H2	30	R1	N-H2	3 days	A1-A1
IV-Casting Age	IV-1/6	30	R1	N-N	4 hours	A1-A1
	IV-28	30	R1	N-N	28 days	A1-A1
	IV-56	30	R1	N-N	56 days	A1-A1
V-Aggregate Size	V-A2	30	R1	N-N	3 days	A1-A2
	V-A3	30	R1	N-N	3 days	A1-A3



Substrate A1-5/8"



Overlay A2-Sand



Overlay A3-3/8"

# EXPERIMENTAL PROGRAM

## Specimen Fabrication



# EXPERIMENTAL PROGRAM

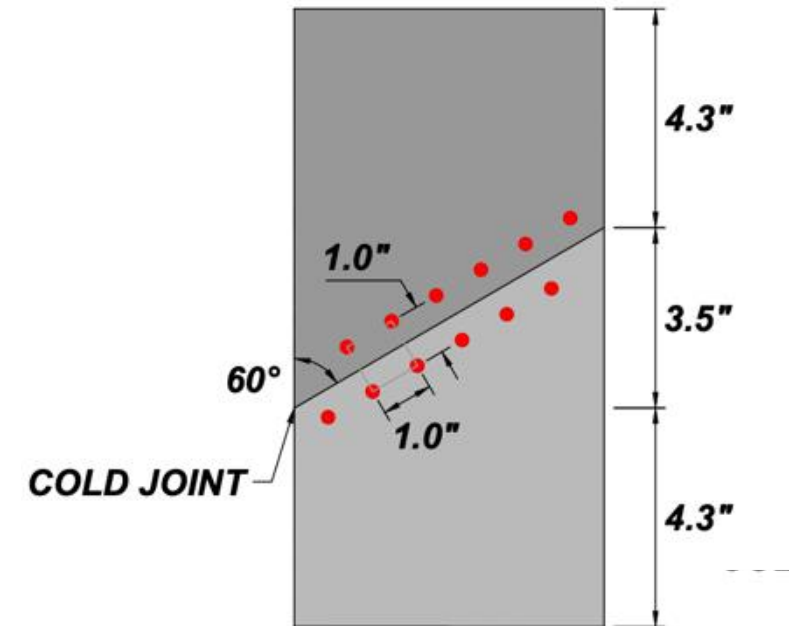
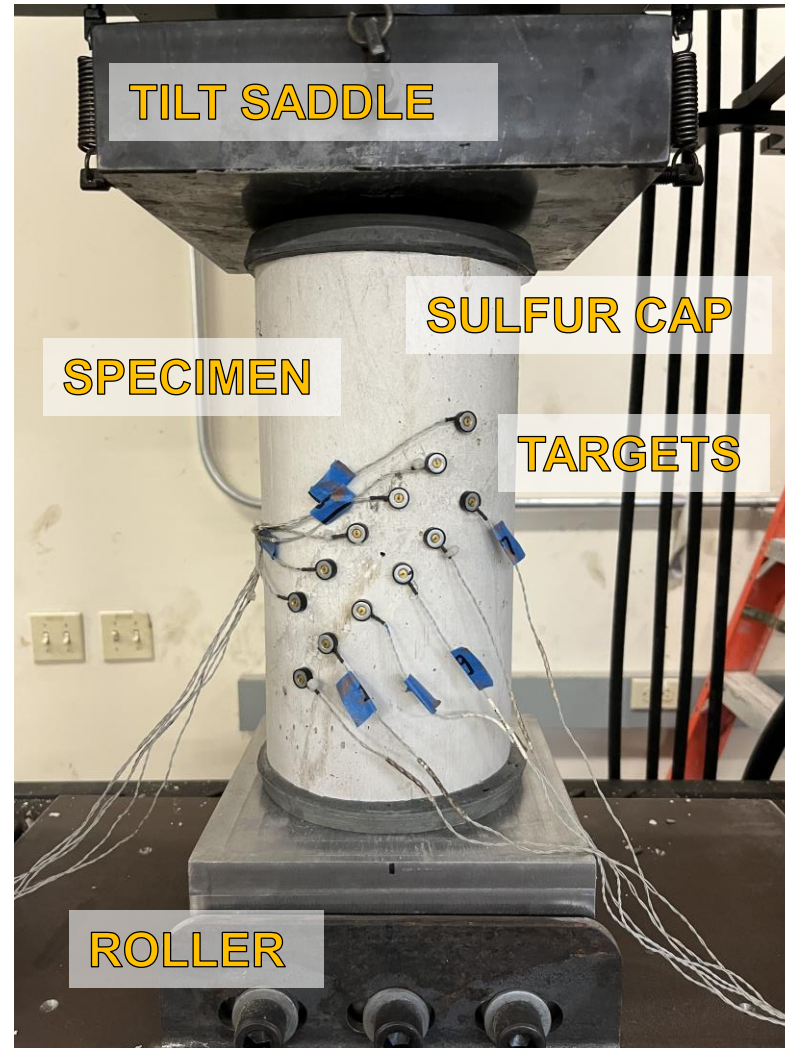
## Test Setup



NDI Optical Tracking System



Sulfur Cap for Contact Surface



Target Arrangement

# EXPERIMENTAL RESULTS

## Failure Mechanisms



Slant shear failure

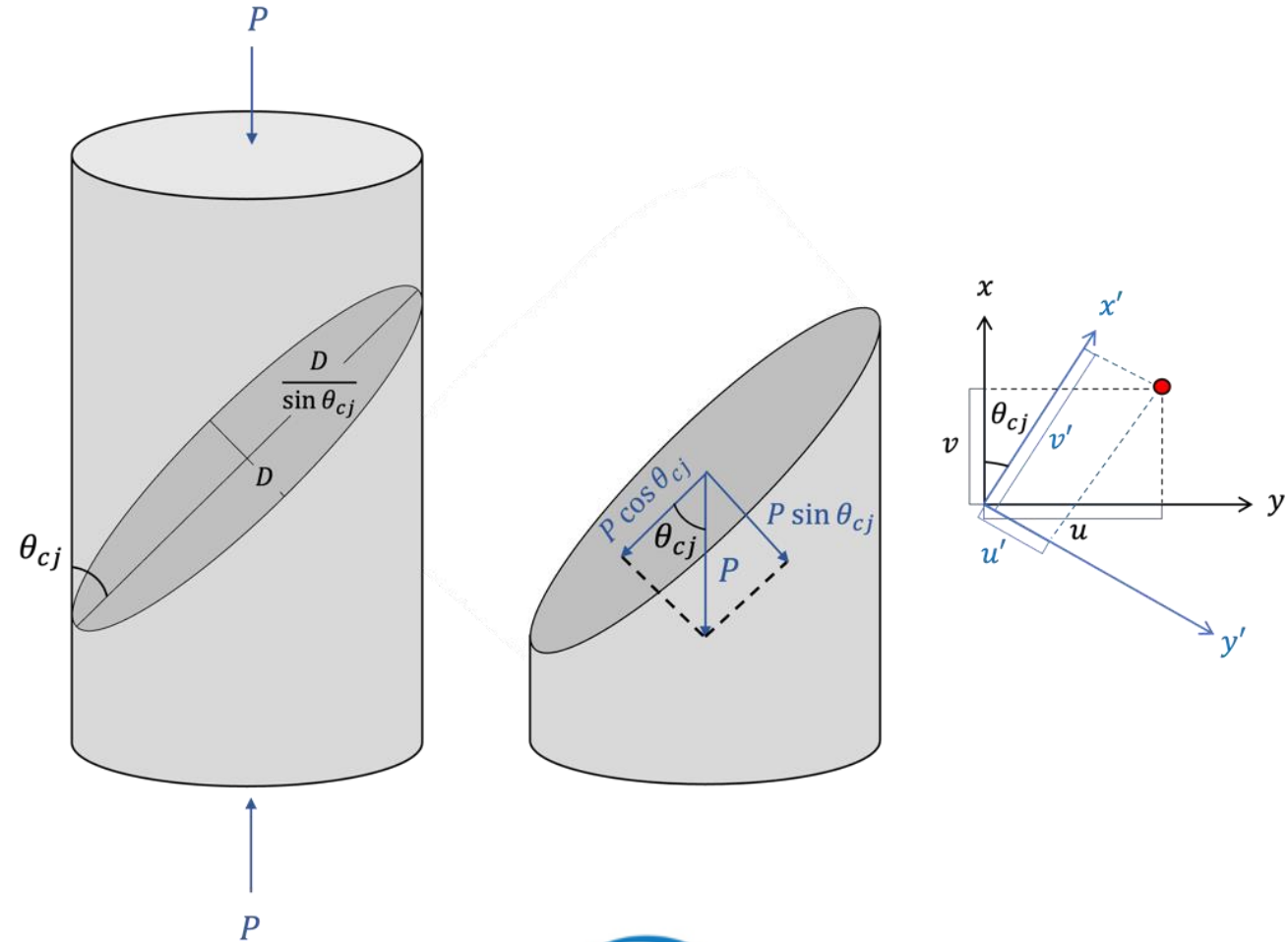


Crushing of concrete



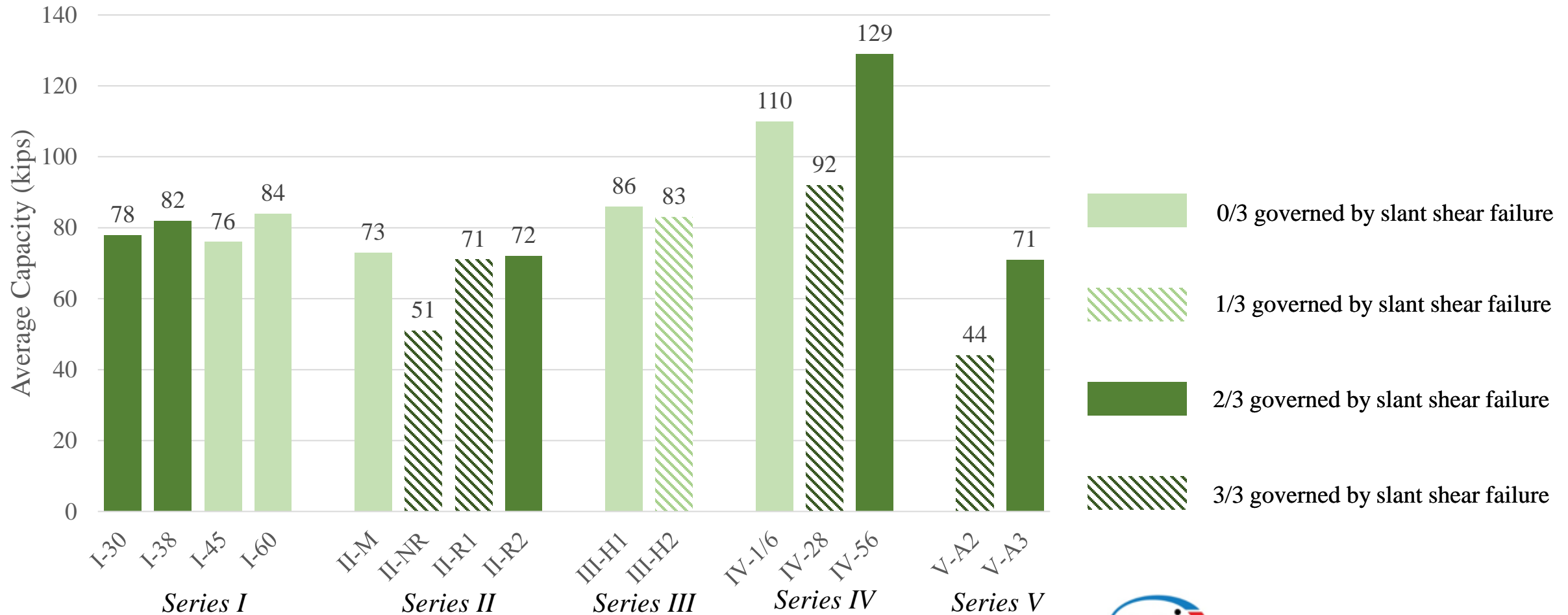
Hybrid failure

## Data Processing Methodology



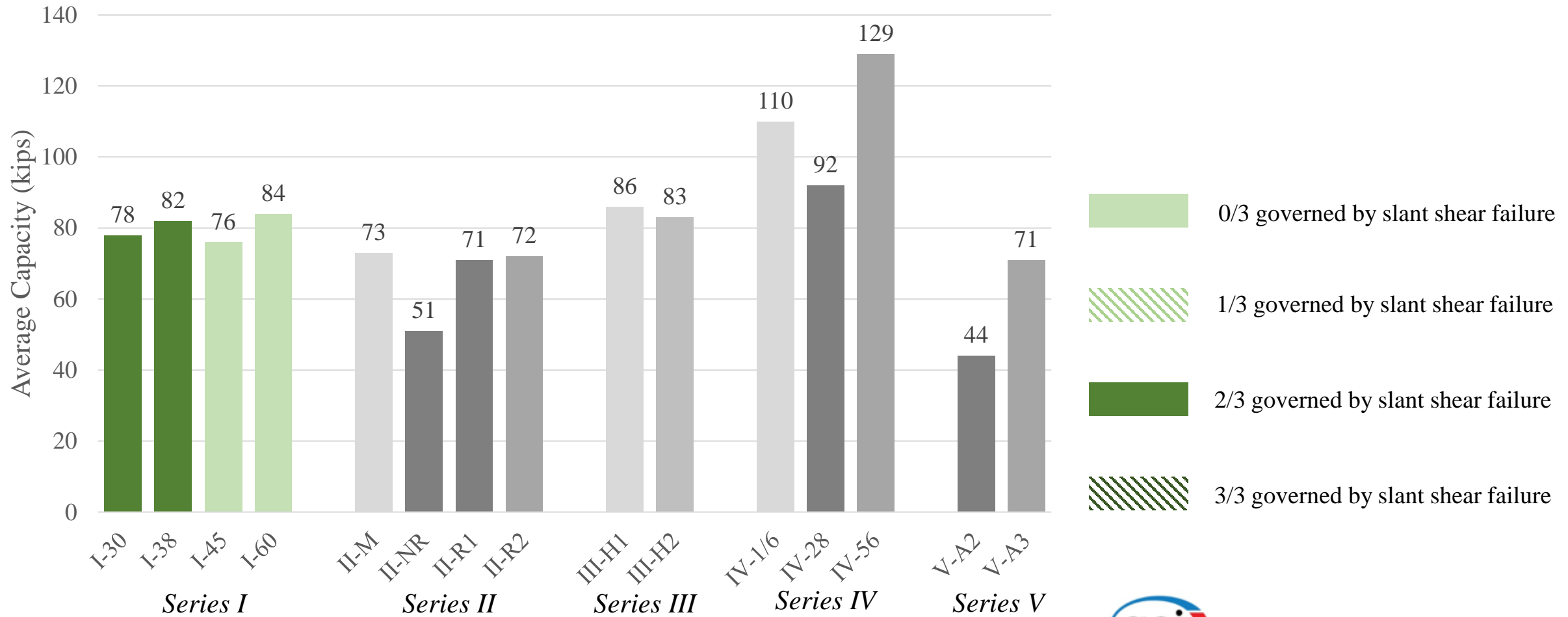
# EXPERIMENTAL RESULTS

## Capacity and Failure Mode



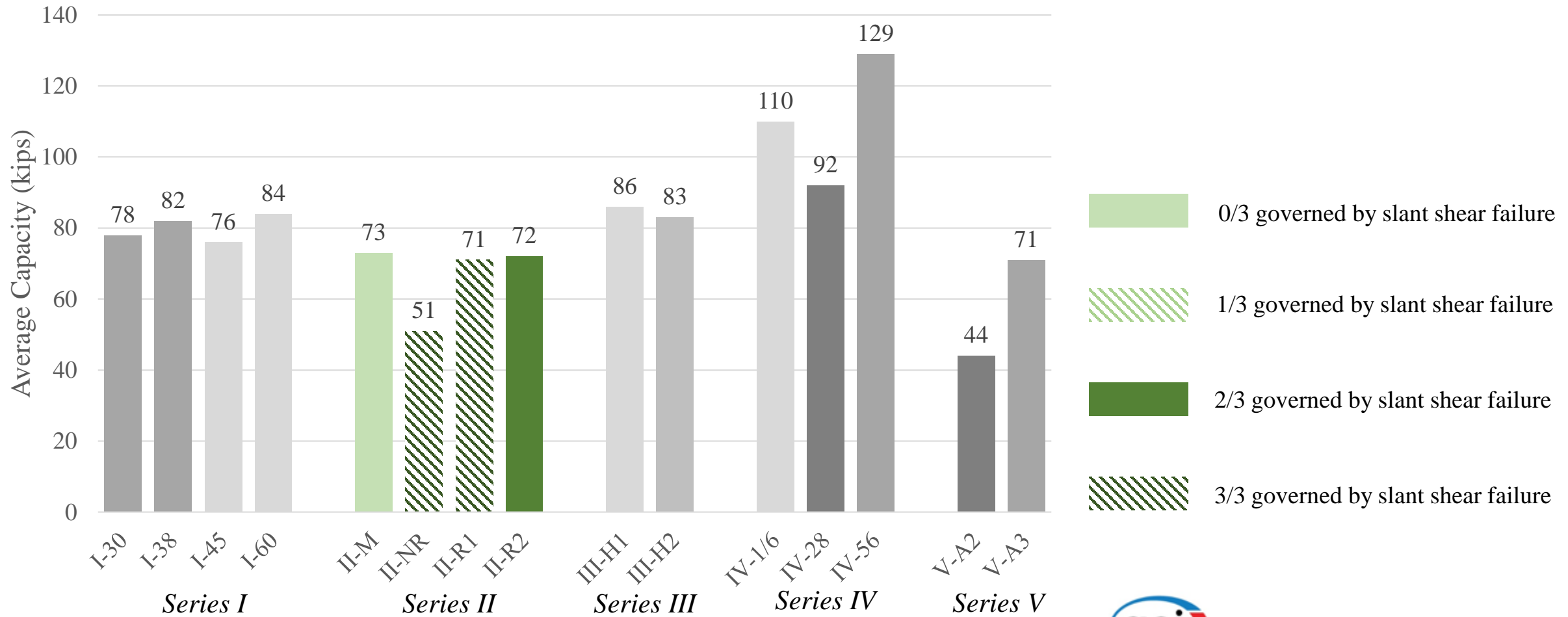
# EXPERIMENTAL RESULTS

## Series I – Inclination: Alternate Failure Mode



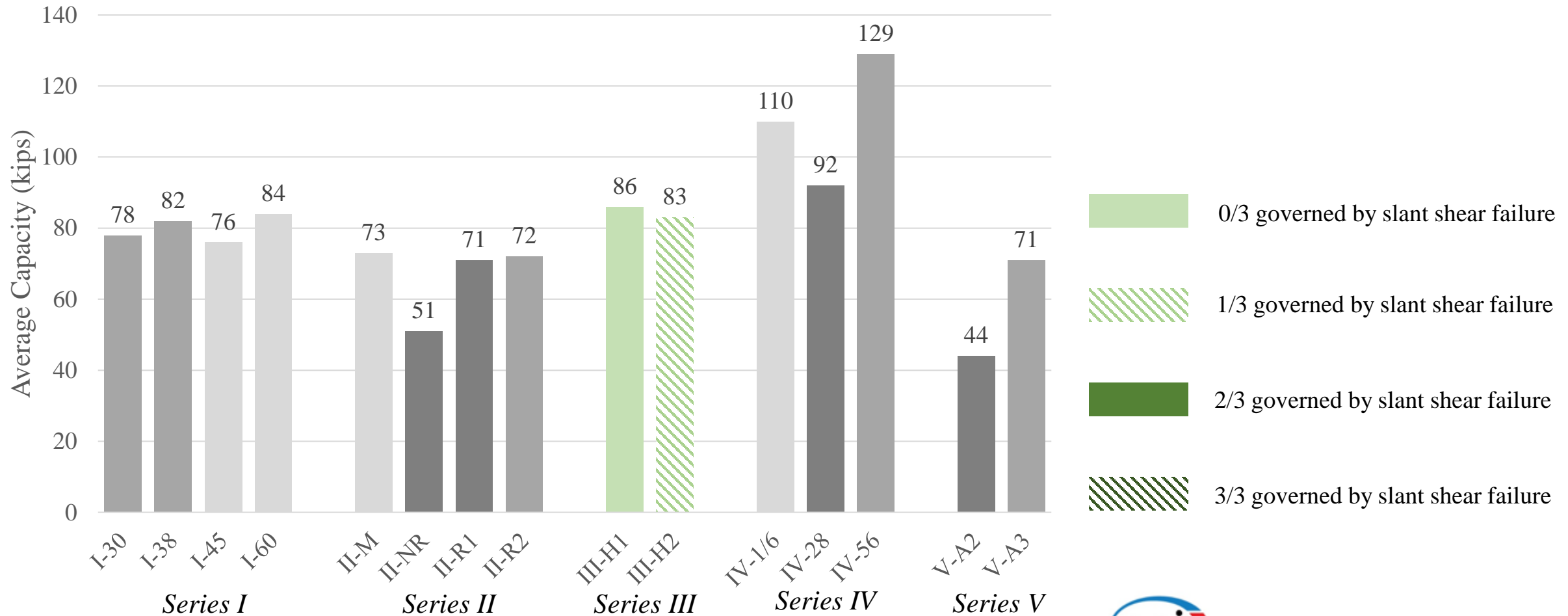
# EXPERIMENTAL RESULTS

## Series II – Interface Roughness: Capacity Decrease with Roughness



# EXPERIMENTAL RESULTS

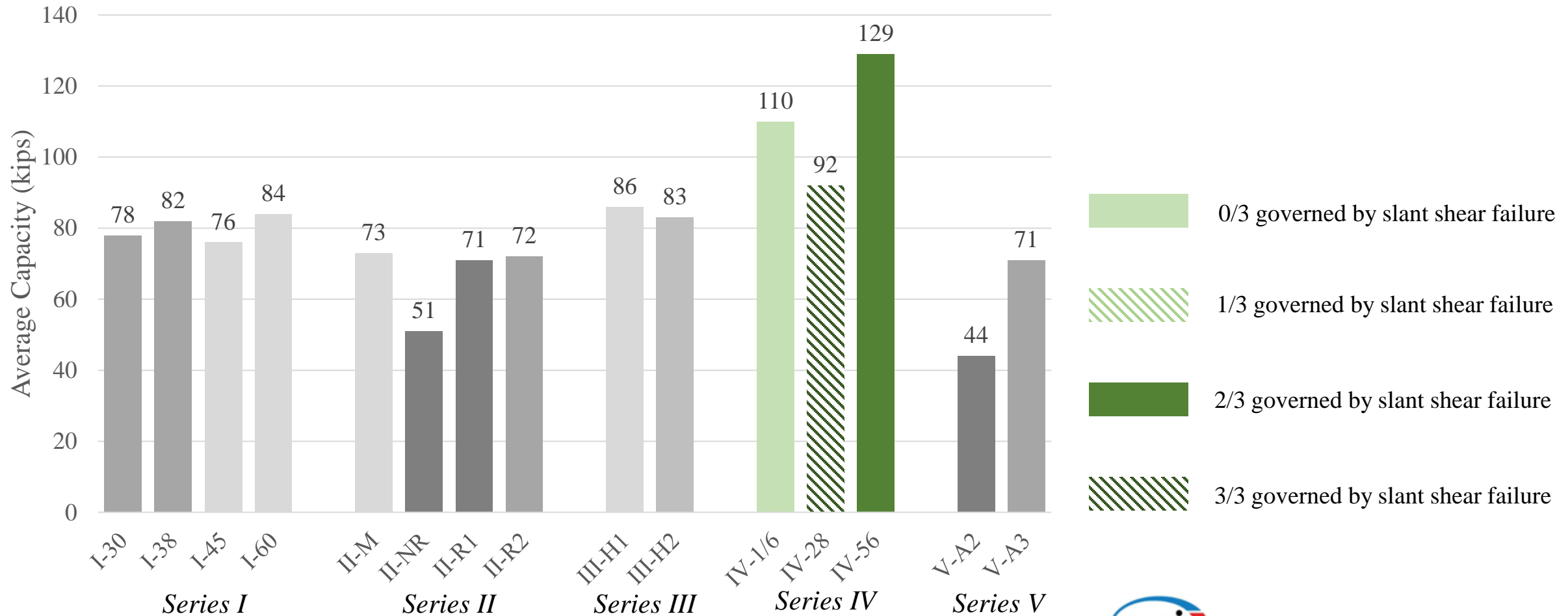
## Series III – Variation of Concrete Strength: Crushing at Weaker Layer





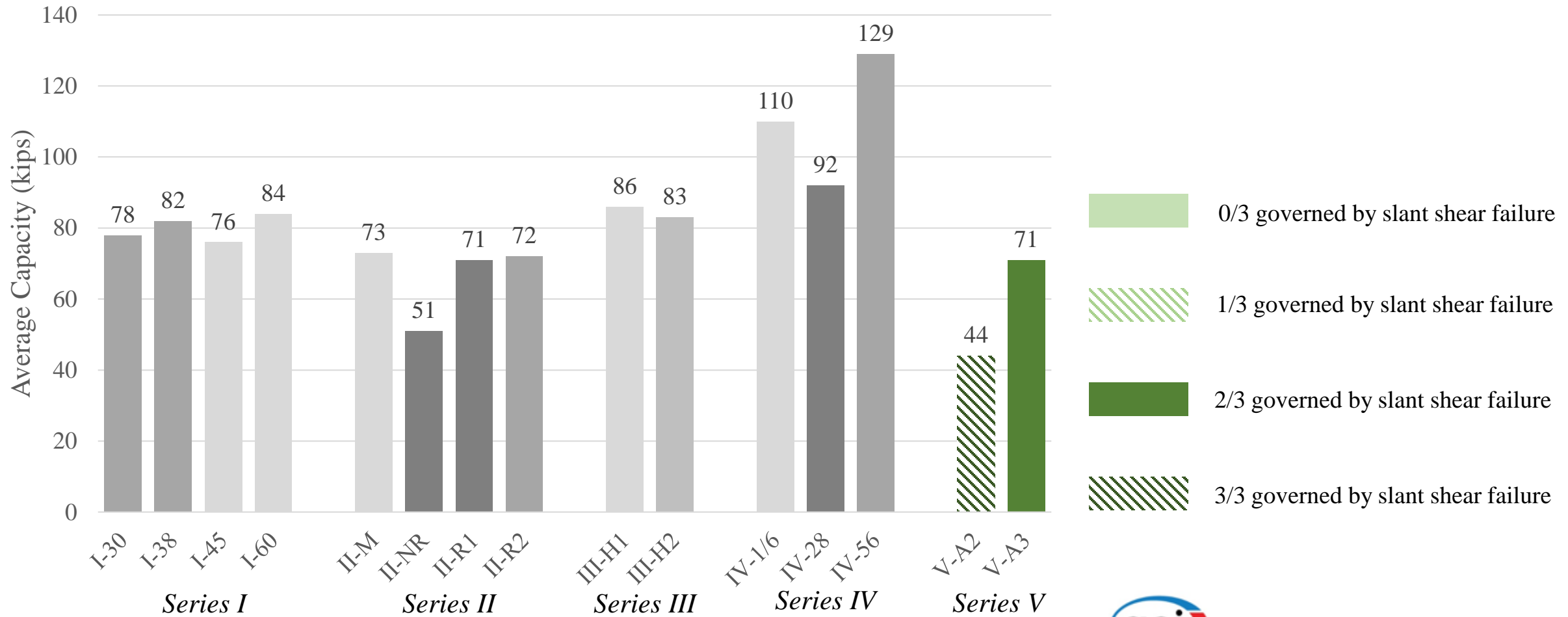
# EXPERIMENTAL RESULTS

## Series IV – Casting Age Difference: Capacity Increase with Age Difference



# EXPERIMENTAL RESULTS

## Series V – Aggregate Size: Capacity Decrease with Aggregate Size



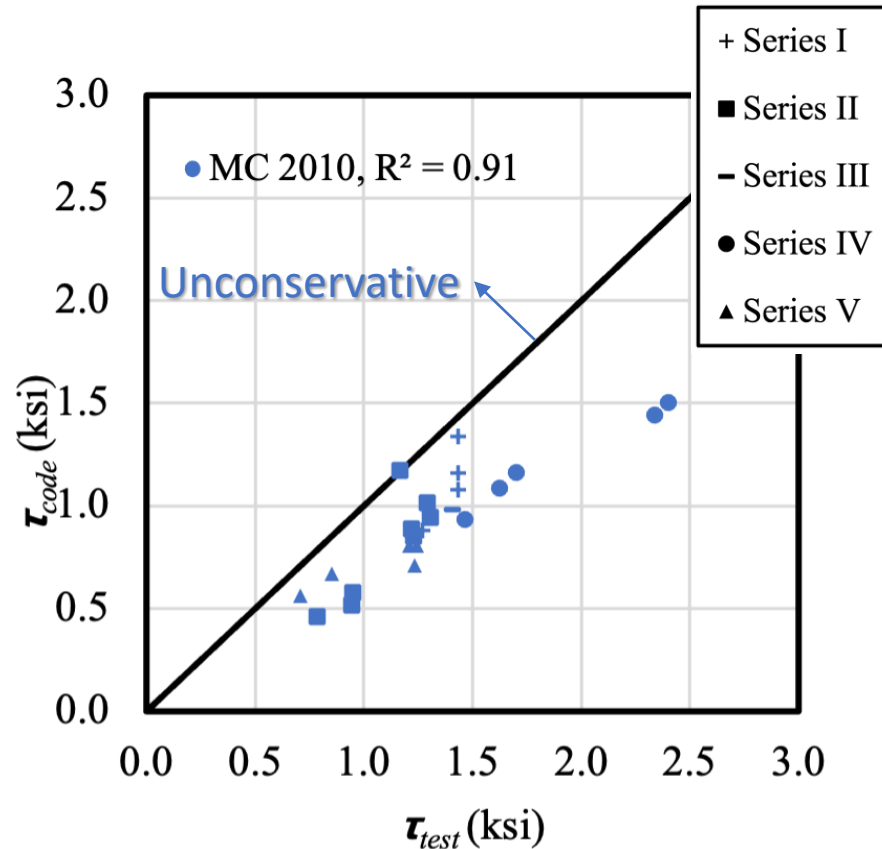
# CODE EVALUATION

Roughening with 0.125-inch amplitude was applied to the specimens

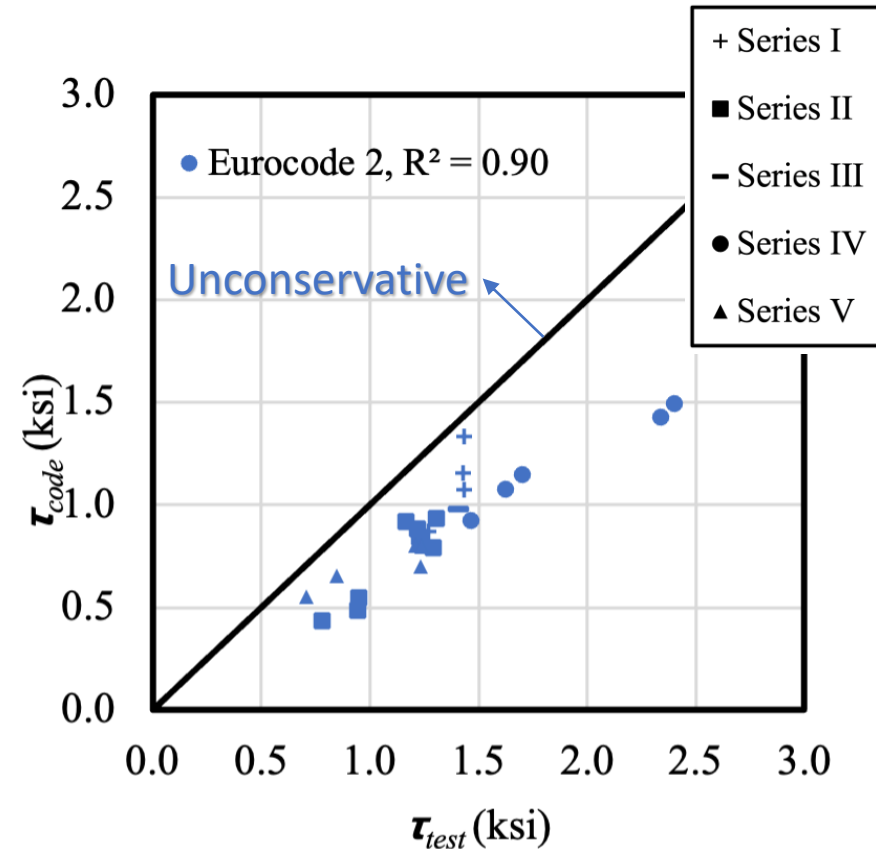
Design code	Amplitude (in.)	$c$ (ksi)	$\mu$	Design Expression
AASHTO LRFD	< 0.25	0.075	0.6	$\tau_n = c + \mu(\rho f_y + \sigma_n)$
	$\geq 0.25$	0.24	1.0	
ACI 318-19	< 0.25	N/A	$0.6\lambda$	$\tau_n = \mu(\rho f_y \sin\alpha + \sigma_n) + \rho f_y \cos\alpha$
	$\geq 0.25$	N/A	$1.0\lambda$	
CSA A23.3:19	< 0.2	0.036	0.6	$\tau_n = \lambda[c + \mu(\rho f_y \sin\alpha + \sigma_n)] + \rho f_y \cos\alpha$
	$\geq 0.2$	0.073	1.0	
Design code	Amplitude (in.)	$c_a$	$\mu$	Design Expression
fib MC2010	< 0.06	0.35	0.6	$\tau_n = c_a f_{ctd} + \mu(\rho f_y \sin\alpha + \sigma_n) + \rho f_y \cos\alpha$
	$\geq 0.06, < 0.12$	0.45	0.7	
	$\geq 0.12$	0.5	0.9	
Eurocode 2	< 0.12	0.2	0.6	$\tau_n = c_a f_{ctd} + \mu(\rho f_y \sin\alpha + \sigma_n) + \rho f_y \cos\alpha$
	$\geq 0.12$	0.4	0.7	

# CODE EVALUATION

## Current Design Code



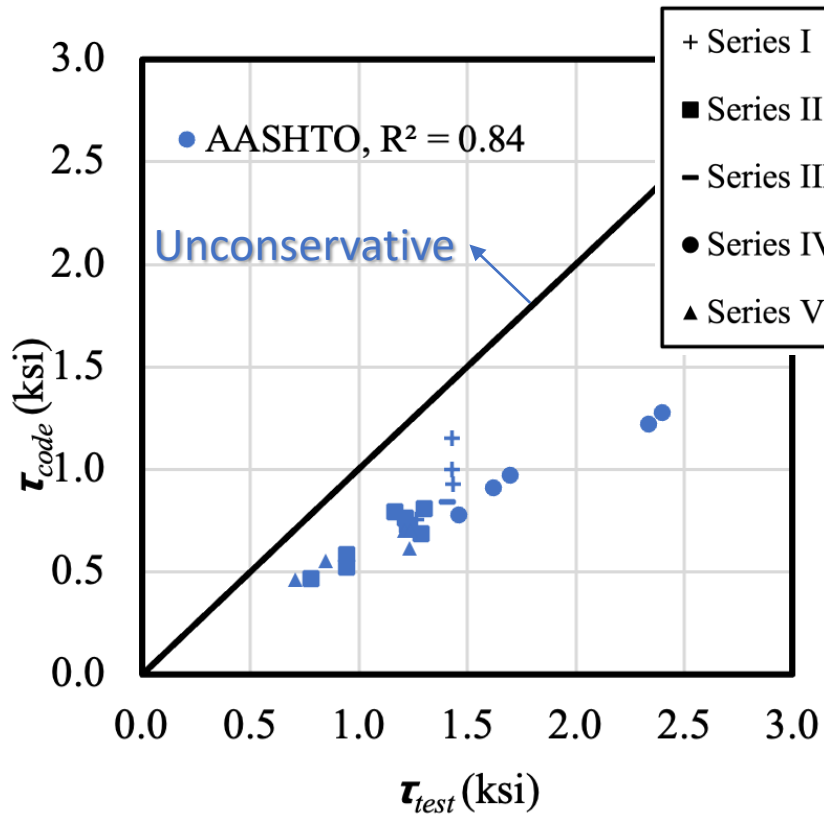
*fib* MC2010



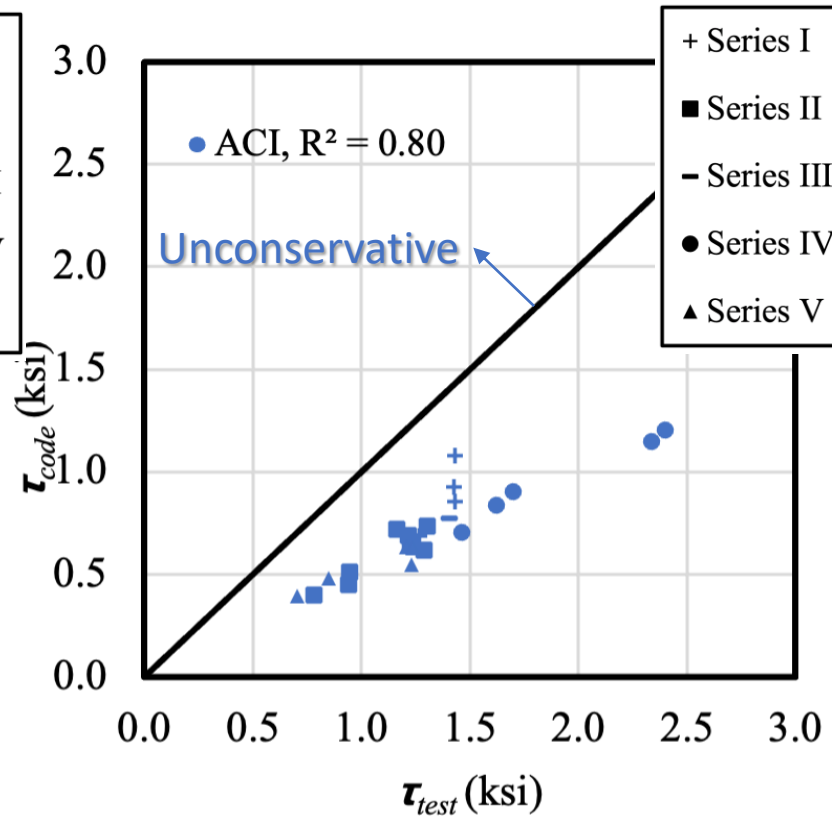
Eurocode 2

# CODE EVALUATION

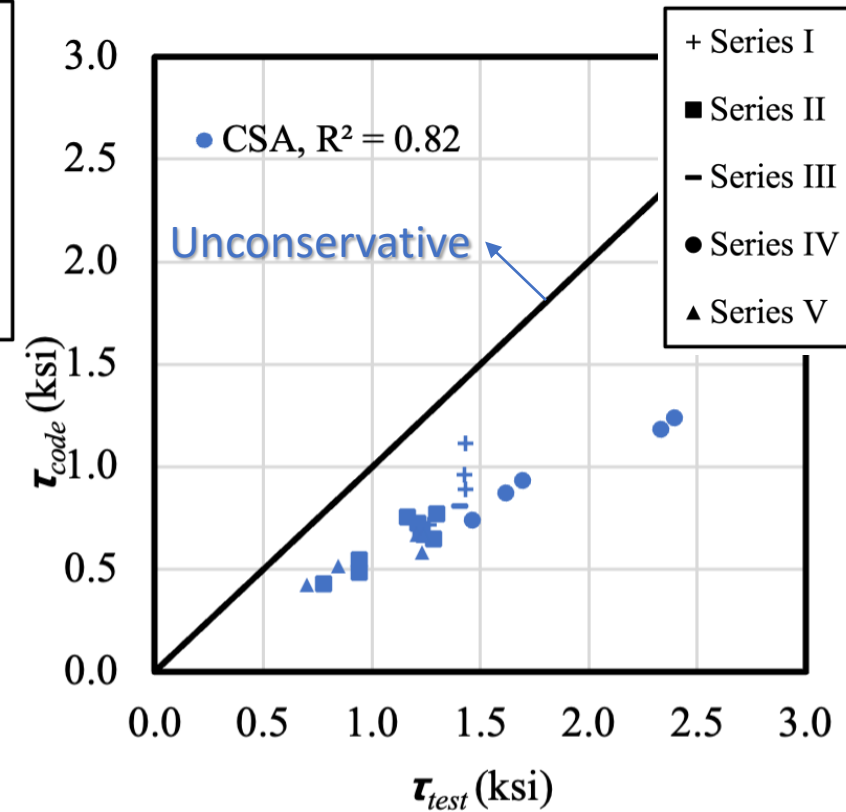
## Current Design Code



AASHTO LRFD (2020)



ACI 318-19



CSA A23.3:19

# CODE EVALUATION

RI Approach - define cold joint as roughened interface disregarding the amplitude

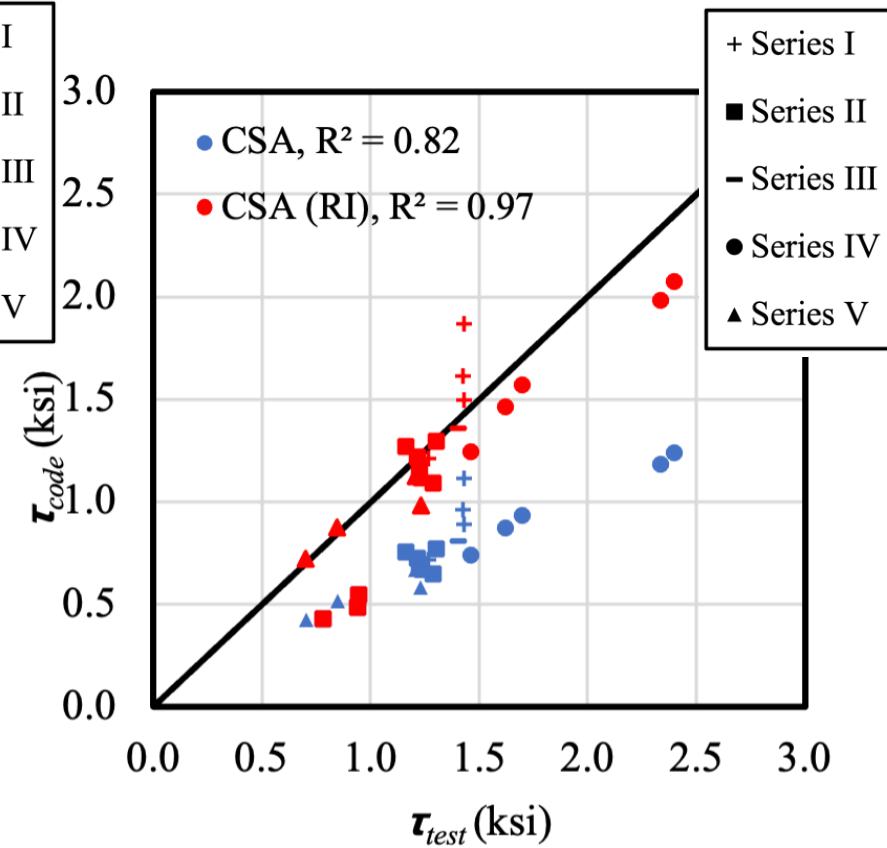
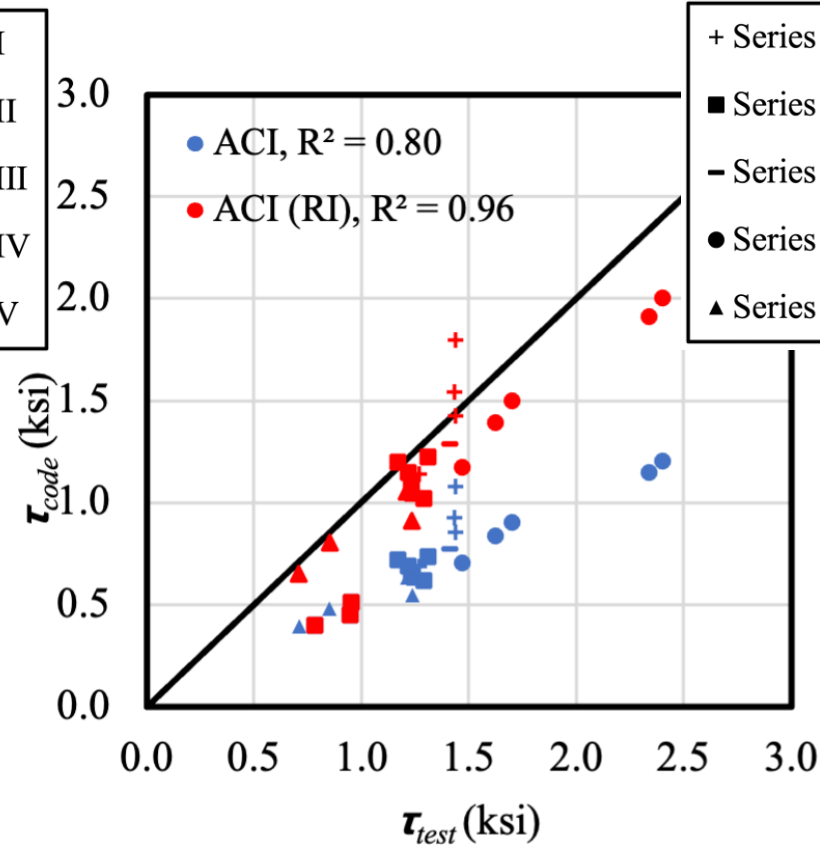
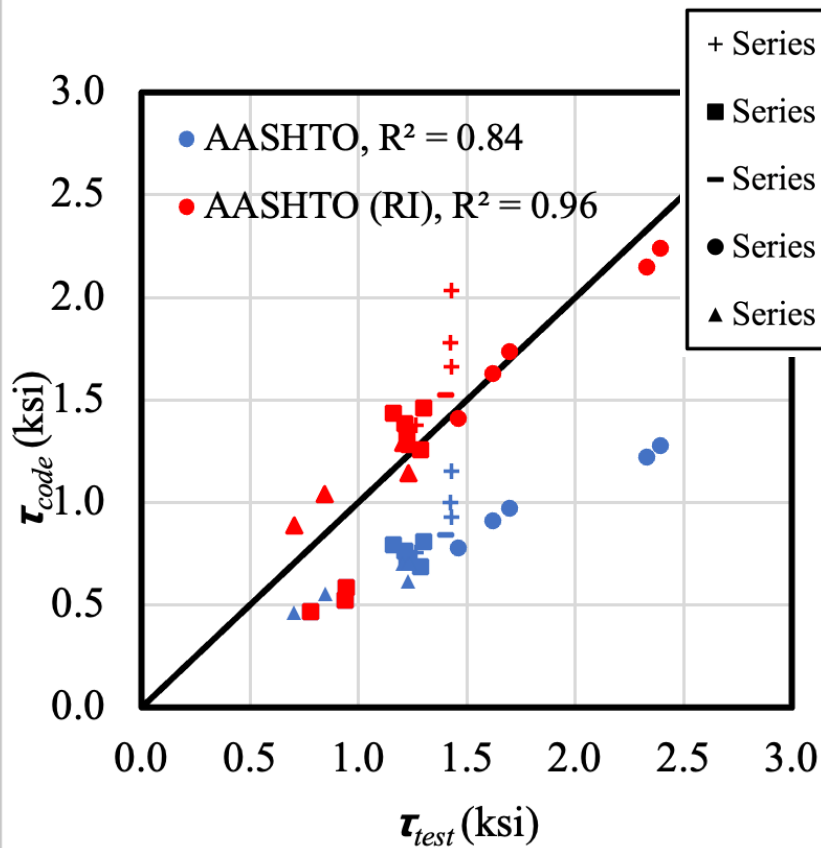
Design code	Amplitude (in.)	$c$ (ksi)	$\mu$	Design Expression
AASHTO LRFD	< 0.25	0.075	0.6	$\tau_n = c + \mu(\rho f_y + \sigma_n)$
	$\geq 0.25$	0.24	1.0	
ACI 318-19	< 0.25	N/A	$0.6\lambda$	$\tau_n = \mu(\rho f_y \sin\alpha + \sigma_n) + \rho f_y \cos\alpha$
	$\geq 0.25$	N/A	$1.0\lambda$	
CSA A23.3:19	< 0.2	0.036	0.6	$\tau_n = \lambda[c + \mu(\rho f_y \sin\alpha + \sigma_n)] + \rho f_y \cos\alpha$
	$\geq 0.2$	0.073	1.0	
Design code	Amplitude (in.)	$c_a$	$\mu$	Design Expression
fib MC2010	< 0.06	0.35	0.6	$\tau_n = c_a f_{ctd} + \mu(\rho f_y \sin\alpha + \sigma_n) + \rho f_y \cos\alpha$
	$\geq 0.06, < 0.12$	0.45	0.7	
	$\geq 0.12$	0.5	0.9	
Eurocode 2	< 0.12	0.2	0.6	$\tau_n = c_a f_{ctd} + \mu(\rho f_y \sin\alpha + \sigma_n) + \rho f_y \cos\alpha$
	$\geq 0.12$	0.4	0.7	

# CODE EVALUATION

## RI Approach

✓ Accuracy of estimations is improved

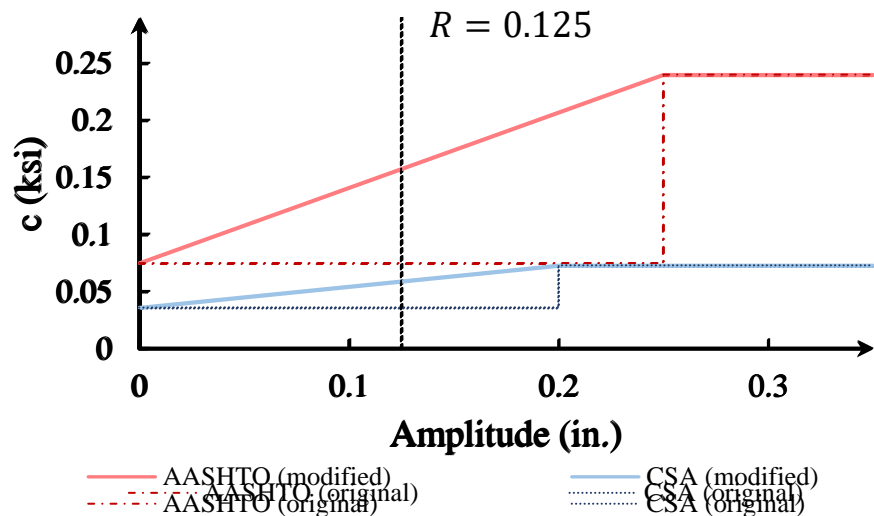
✗ Numerous unconservative cases were observed



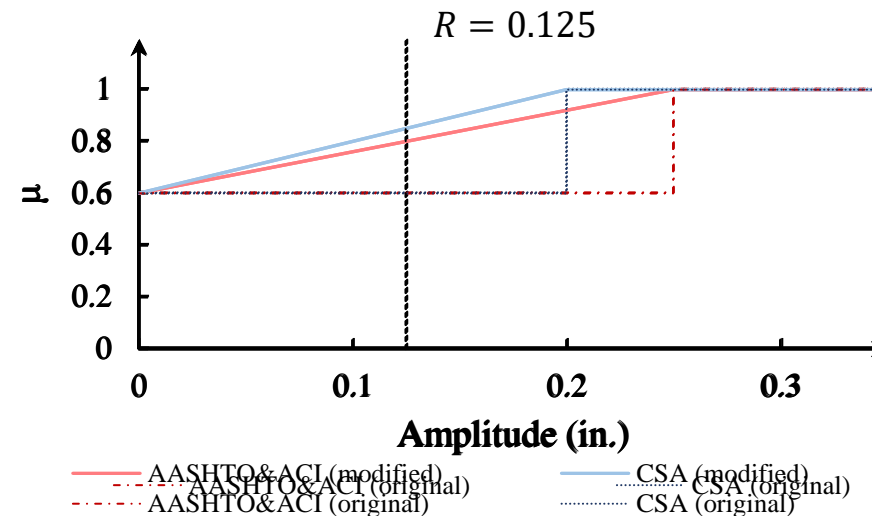
# CODE EVALUATION

## LIF Approach - factors are linear interpolated based on the roughness amplitude

Design code	Amplitude (in.)	c (ksi)	$\mu$	Design Expression
AASHTO LRFD	< 0.25	0.075	0.6	$\tau_n = c + \mu(\rho f_y + \sigma_n)$
	$\geq 0.25$	0.24	1.0	
ACI 318-19	< 0.25	N/A	$0.6\lambda$	$\tau_n = \mu(\rho f_y \sin\alpha + \sigma_n) + \rho f_y \cos\alpha$
	$\geq 0.25$	N/A	$1.0\lambda$	
CSA A23.3:19	< 0.2	0.036	0.6	$\tau_n = \lambda[c + \mu(\rho f_y \sin\alpha + \sigma_n)] + \rho f_y \cos\alpha$
	$\geq 0.2$	0.073	1.0	



Cohesion Factor



Friction Factor

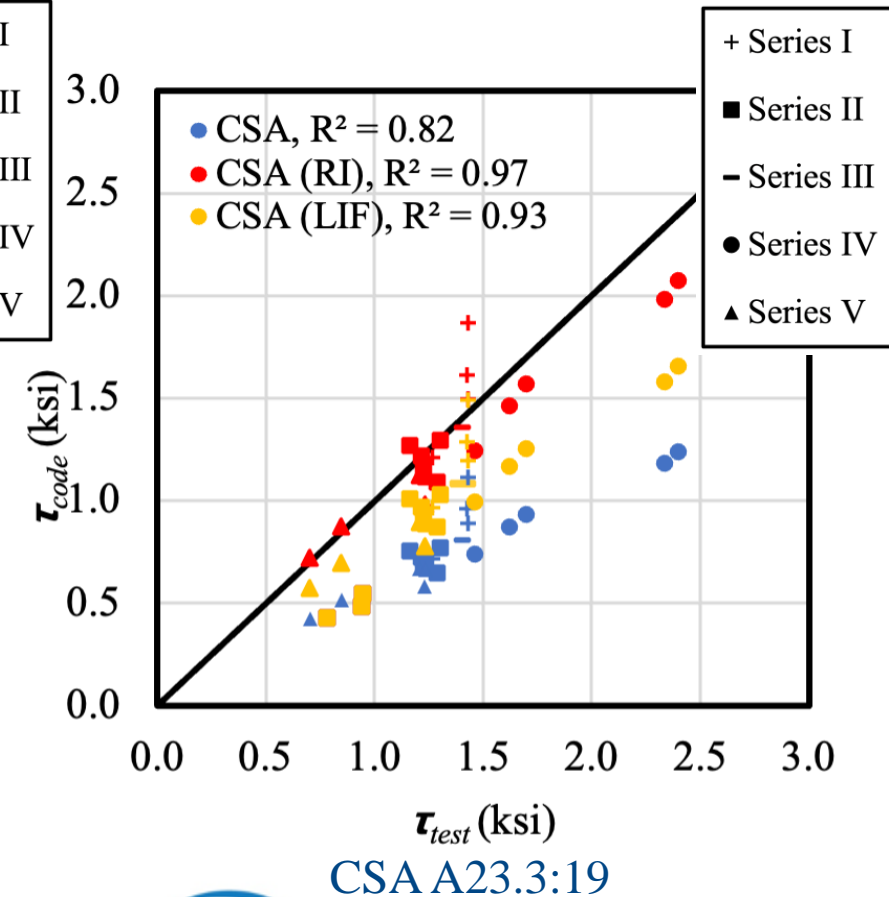
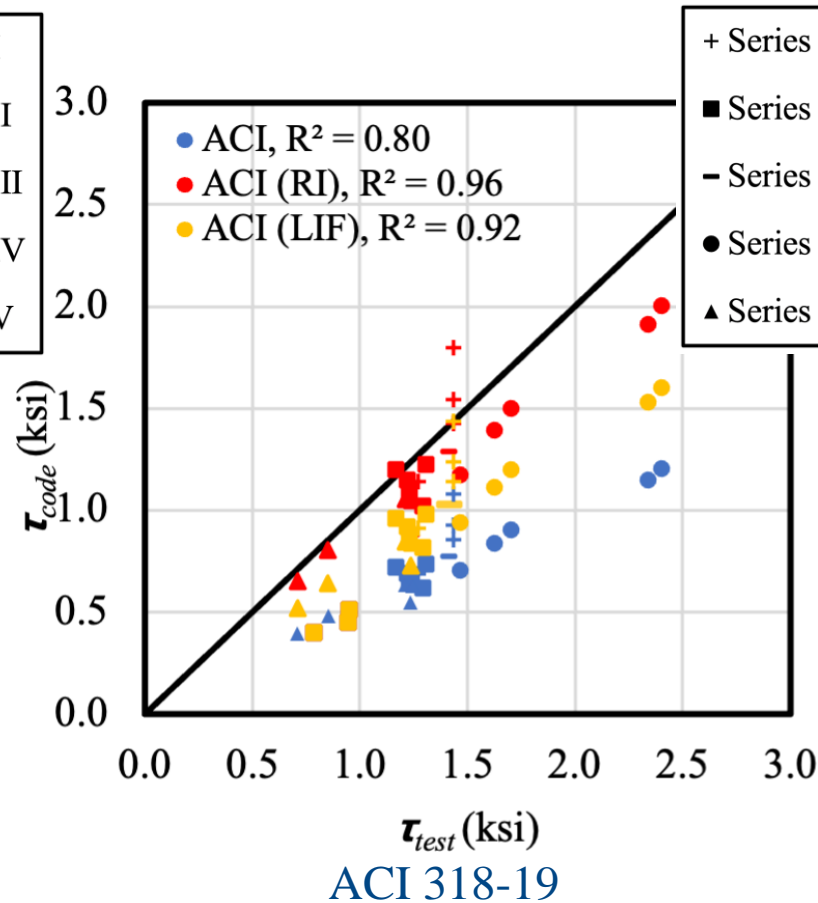
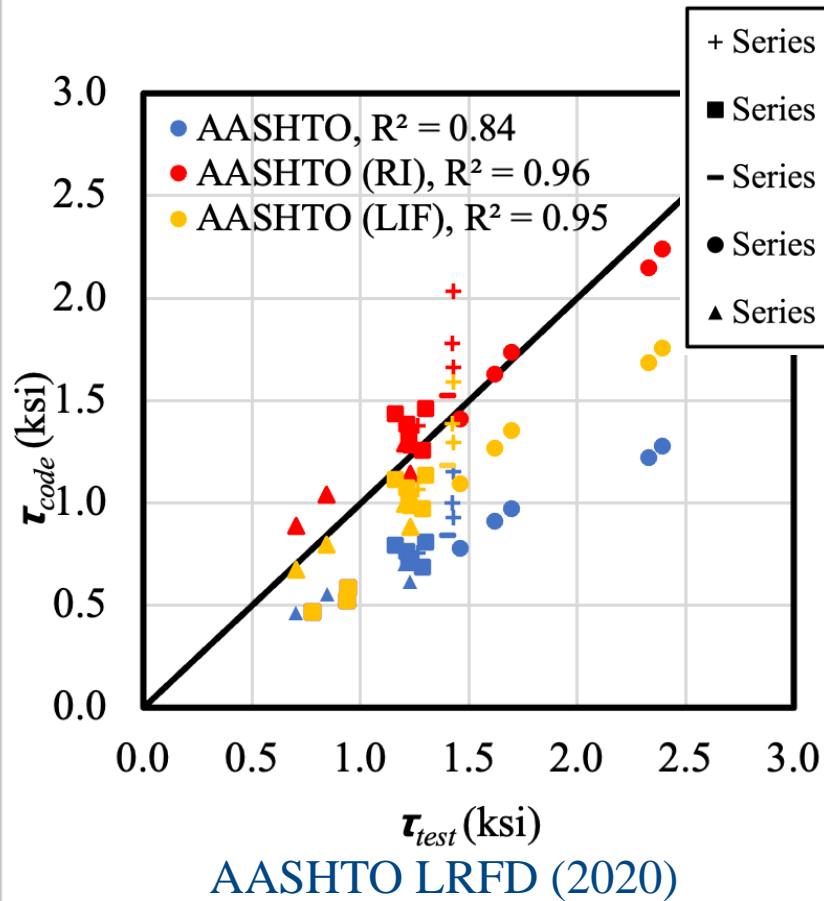


# CODE EVALUATION

## LIF Approach

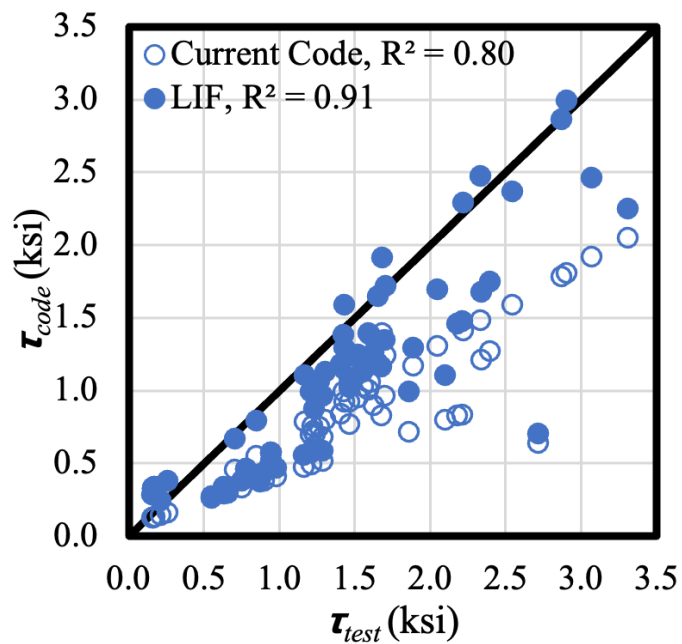
✓ Accuracy of estimations is improved

✓ Only a few unconservative cases were observed

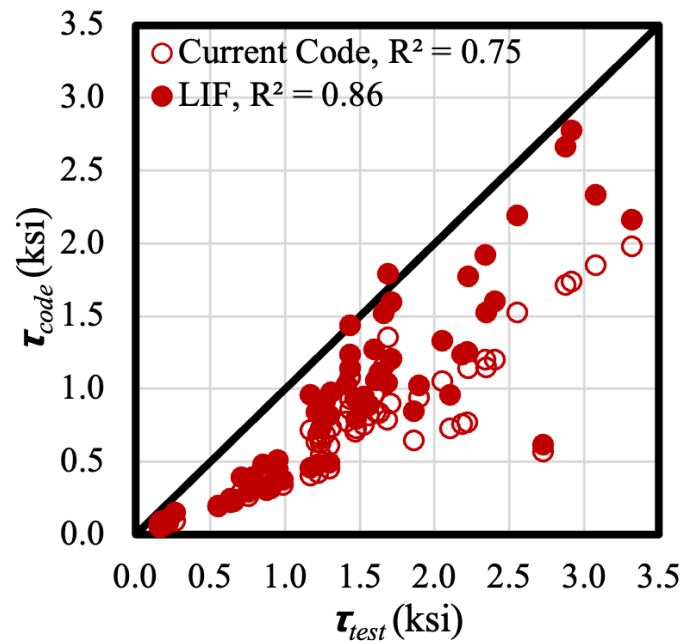


# DATABASE ANALYSIS

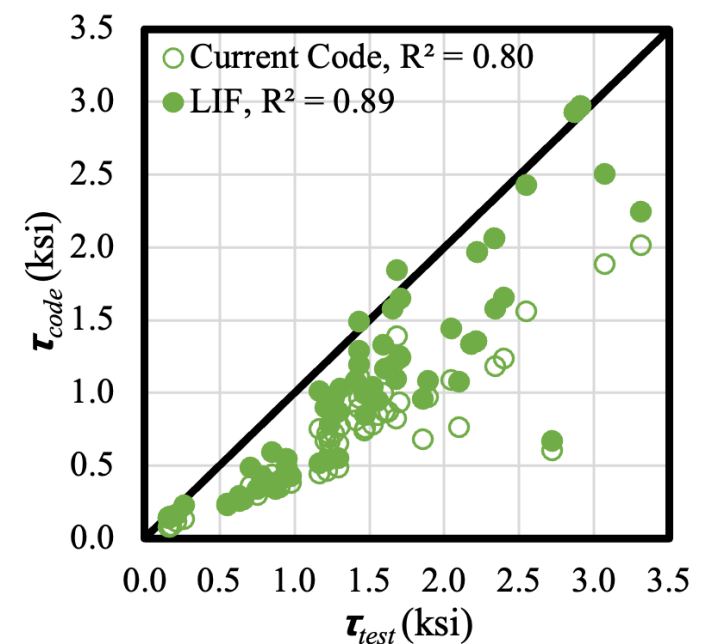
Source	Number of Specimens	Geometry	$\theta_{cj}$ (°)	$R_a$ (in.)	D (in.)	Roughening Approach
Figueiredo et al.	75	cylindrical	30	0.034 – 0.22	5.51	hand-scrubbing; vibrating
Santos & Júlio	150	prismatic	30	0.01 – 0.048	5.91	wire-brushing; sandblasting; shotblasting; hand-scrubbing
Diab et al.	150	cylindrical	30	0.12, 0.24	5.91	patterned groves
Saldanha et al.	12	prismatic	30	0.197, 0.59	5.91	hand-scrubbing; patterned groves
Hu et al.	96	cylindrical	30, 40	0.12, 0.24	2.77	patterned groves



AASHTO LRFD (2020)



ACI 318-19



aci CONCRETE CONVENTION  
CSA A23.3:19

# CONCLUSIONS & FUTURE WORK

## CONCLUSIONS

- Applying intentional roughening and using larger aggregate size improve the capacity of cold joint significantly.
- The control failure mode switch from slant shear to compression failure by increase the inclination.
- Cold joint capacity estimated by LIF demonstrate better alignment with the experimental results.
- LIF is more impactful on intentionally roughened interface with higher shear capacity.

## FUTURE WORK

- Large scale slant shear column
- Deep beam with cold joint
- Drill-shaft footing with expansion
- Shear-slip relationship of interface for FEA



# THANK YOU!



## ACKNOWLEDGEMENT

This research is sponsored by  
Texas Department of Transportation

## CONTACT INFORMATION

Brandon Li  
[bl28458@my.utexas.edu](mailto:bl28458@my.utexas.edu)

Andrea Campos Sanchez  
[andrea.campossanchez@utexas.edu](mailto:andrea.campossanchez@utexas.edu)

THE WORLD'S GATHERING PLACE FOR ADVANCING CONCRETE

